Experimental Techniques (2018) 42:523–532
https://doi.org/10.1007/s40799-018-0256-z

A New Method of Creating High-Temperature Speckle Patterns and Its Application in the Determination of the High-Temperature Mechanical Properties of Metals

Y.J. Hu[1] · Y.J. Wang[1] · J.B. Chen[1] · J.M. Zhu[1]

Received: 26 July 2017 / Accepted: 10 May 2018 / Published online: 5 June 2018
© The Society for Experimental Mechanics, Inc 2018

Abstract
Speckle techniques, such as DIC (Digital Image Correlation) and DSP (Digital Speckle Photography), are frequently used to determine the high-temperature mechanical properties of materials. Speckle techniques require the creation of a random speckle pattern on the surface of the specimen. The most commonly used approach to creating a high-contrast speckle pattern is to spray a layer of black paint particles on a white background. However, in a high-temperature environment, the paint particles tend to peel off or burn off. In this paper, we present an approach that uses a novel laser-engraving technology, where the created speckles will sustain temperatures as high as the melting temperature of the specimen. The size, density, depth and distribution of the speckles can be controlled to suit a particular situation. Since the pattern is part of the specimen, it will never disappear, until the melting temperature of the metal is reached. As an application, we used the technique to determine the elastic modulus of Ti up to 600°C and tungsten up to 1000°C.

Keywords DIC · Speckles · High-temperature testing · Mechanical property of metals · Material testing

Introduction

The use of a random speckle pattern for quantitative displacement/strain analysis is a major advance in experimental mechanics. There have been two parallel developments: the ubiquitous DIC (Digital Image Correlation) method [1–6] and the DSP (Digital Speckle Photography) technique [7]. Although the two methods have identical physics, their mathematical approaches are different. The former uses a straightforward correlation calculation in the spatial domain, whereas the latter first performs a Fourier transform of the speckle pattern and subsequently performs the correlation calculation in the spectrum domain [7–10].

Most applications of the speckle technique are in a room temperature environment. However, in recent years, the high-temperature usage of the speckle technique has seen rapid development because of the demand to characterize the mechanical properties of materials, such as metals, for applications in high-temperature environments, such as the combustion chamber of a jet engine.

Extensive experimental studies using the DIC method have been conducted on the mechanical characteristics of materials at high temperature [11–23], where painted speckles [11–13], laser speckles [14, 15] and high-temperature-resisting coat speckles [16–23] are used. High-temperature material characteristics, such as the tensile strength, yield strength, elastic modulus, thermal expansion coefficient, and creep coefficient, have been studied. However, the application of the DIC method for high-temperature strains and deformation measurements remains challenging for two reasons [16, 22]: (1) the ability of the coating to resist heat and to withstand deformation without cracking or peeling; and (2) the radiation from the specimen's surface at high temperature. Chen et al. [23] used a monochromatic light with a different wavelength from the radiating spectrum from the specimen's surface to overcome the difficulties of surface radiation due to high temperature. A coating material that consists of amorphous precipitated silica and titanium dioxide has been proven to have outstanding performance in high-temperature DIC tests.

✉ Y.J. Hu
huyujia@126.com

[1] School of Mechanical Engineering, University of Shanghai for Science and Technology, Shanghai 200093, China

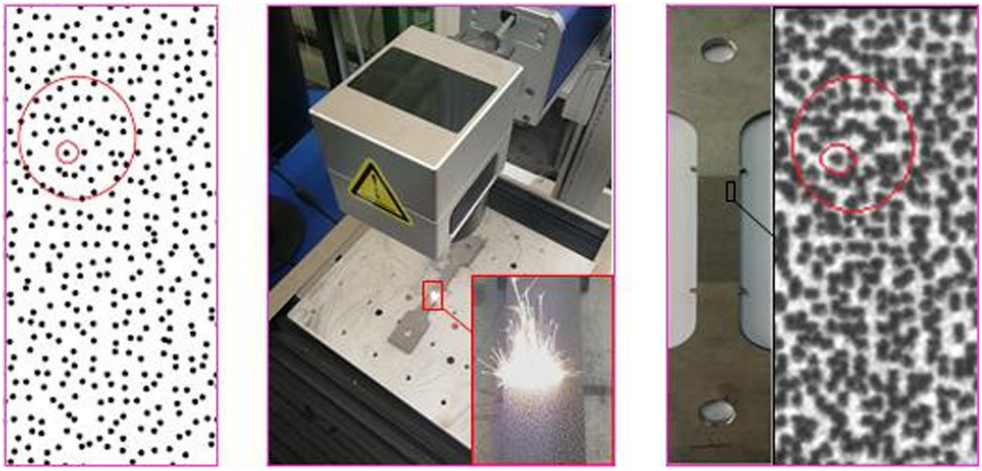

Fig. 1 Laser engraving machine and engraved speckles: (**a**) computer-generated speckle pattern; (**b**) laser engraving system; (**c**) laser-engraved speckle pattern based on the computer input

In this paper, we present a new approach to create high-temperature speckle patterns using a novel laser engraving technology. Speckle patterns of various sizes, densities, depths and distributions can be engraved onto the surface of a specimen without noticeably damaging the material itself. Such a technique can be applied to create speckles on the surfaces of the metal materials and the nonmetal materials, such as FRP and indium oxide. Since the speckle pattern is a part of the specimen, it will never come off the specimen surface until the melting temperature of the material is reached. We have successfully applied this technique to measure Young's modulus and Poisson's ratio of a titanium alloy up to 600°C and of tungsten up to 1000°C.

Technique of Creating High-Temperature Speckle Patterns by Laser Engraving

An engraving technique to directly produce a random speckle pattern onto the surface of a specimen should be developed because most "added-on" speckle patterns (such as spraying on high-temperature paint particles) tend to fail before the specimen reaches its intended testing temperature. Engraved speckles will remain on the specimen until the specimen itself fails (i.e., melts) because the speckles are part of the specimen. The technique that we developed consists of the following steps:

(1) Generate random two-dimensional coordinates of points in the X-Y plane. The density and distribution of the speckles can be controlled.
(2) Assign a radius to each speckle point; the size of the speckles can be controlled.
(3) Generate a computer-generated speckle pattern by two-dimensional coordinates of random points and the radius of the speckles. A typical computer-generated speckle pattern is shown in Fig. 1(a).
(4) Import the computer-generated speckle pattern into a specially designed fiber laser engraving system, as shown in Fig. 1(b).
(5) Adjust the output power and exposure time of the fiber laser engraving system. A laser-engraved speckle pattern can be created, as shown in Fig. 1(c); the depth of the speckle pattern can be controlled. With the current system, the smallest speckle size that we can produce is approximately 5 μm. The main technical parameters of the laser engraving system are listed in Table 1.

The laser engraving technique can be applied to create speckles on both metal and nonmetal materials, such as FRP and indium oxide, as shown in Fig. 2, where the enlarged speckle patterns are captured by a CCD camera. Moreover, this method can be applied to a curved surface by using a rotating shaft in the laser engraving system, as shown in Fig. 3. An actual speckle pattern on the curved surface of a mild steel is shown in Fig. 2(d).

Table 1 Technical parameters of the laser engraving system

Output power	Galvo scanning velocity	Engraved range	Power stability
20 W	7000 mm/s	100 mm~110 mm	1.2%

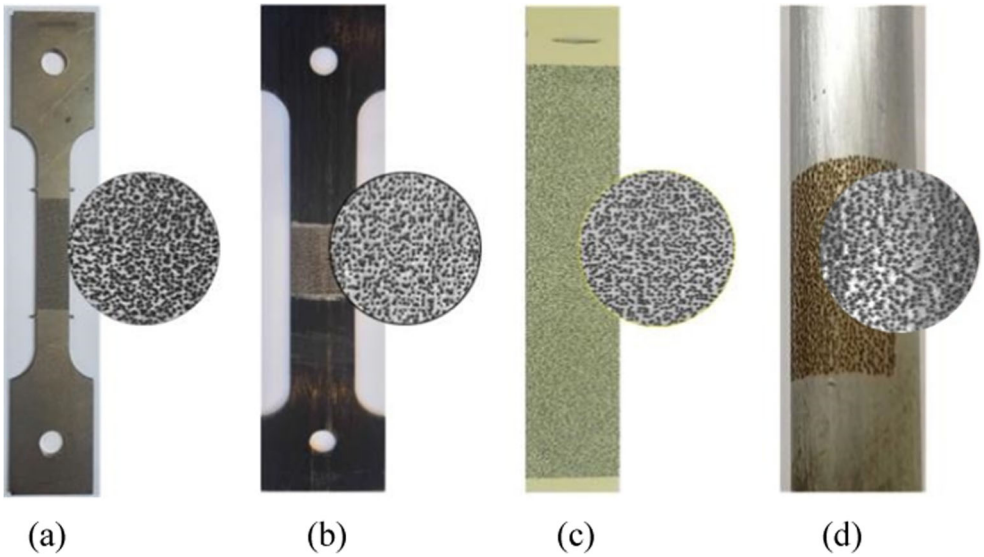

Fig. 2 Speckle patterns on metallic and nonmetallic materials: (**a**) Ti alloy, (**b**) FRP, (**c**) indium oxide and (**d**) curved surface of a mild steel

High-Temperature Measurement System

To satisfy the requirements of a non-contact measurement at high temperature, a new measurement system is designed as schematically shown in Fig. 4. This system consists of four subsystems: (1) a universal testing machine housed in a vacuum chamber; (2) a heating system, which includes a high-temperature cylindrical vacuum furnace, a high-temperature vacuum pump, and associated measuring sensors; (3) a lighting system with multiple green LED illuminators; and (4) a digital image acquisition system with two symmetrically placed CCD cameras. Each camera is equipped with a 532-nm narrow band (10-nm) filter to block out ambient light and to overcome difficulties of the radiation from the specimen's surface. A detailed high-temperature experimental device with important subsystems is shown in Fig. 5.

The cylindrical high-temperature vacuum furnace is heated by heating the wires, and the specimen is located in the middle of the cylindrical high-temperature vacuum furnace to guarantee that the specimen has uniform heating, as shown in Fig. 5(c). A B-type thermocouple is used to test the temperature of the specimen. Its limiting temperature is 1300°C, with a measurement resolution of 0.1°C. After reaching the required temperature of the experiment, the power is maintained for 2 or 3 min until the temperature is stable, and the experiment is subsequently begun.

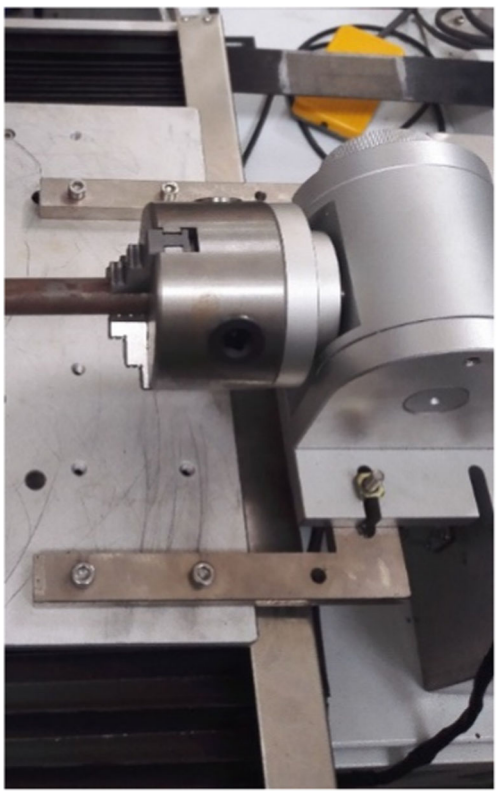

Fig. 3 A rotating shaft in the laser engraving system

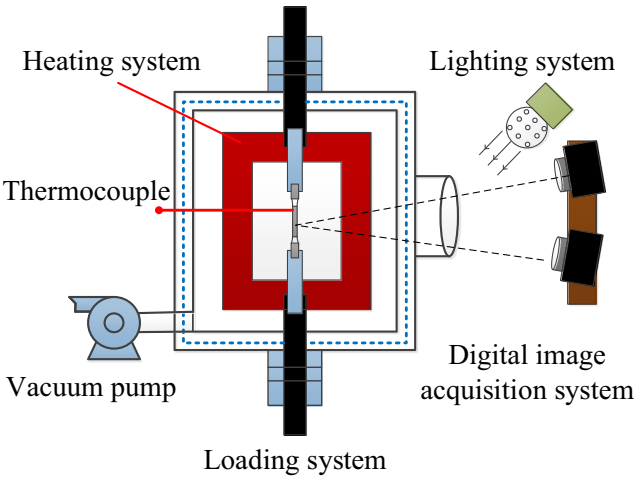

Fig. 4 High-temperature deformation measurement system

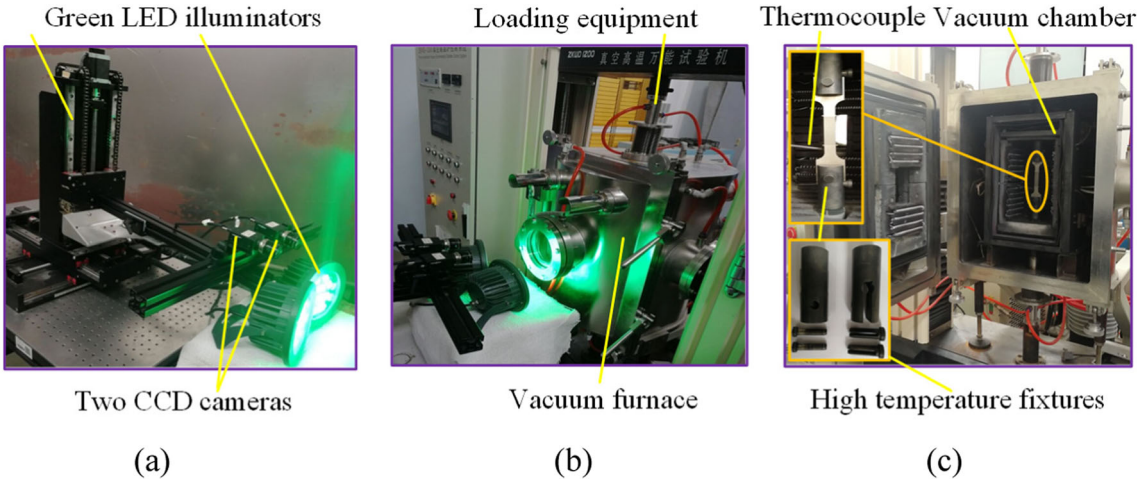

Fig. 5 High-temperature experimental device with important subsystems: (**a**) lighting and image acquisition systems; (**b**) heating and loading systems; (**c**) vacuum chamber, specimen and high-temperature fixtures

An image acquisition with an analysis software (VIC-3D) is used to obtain the displacement and strain distributions at the surface of a specimen. Only one camera is required for the plane 2D situation. However, because the specimen tends to twist under loading, we found that the 3D-DIC system with two cameras yields much better results. Unless otherwise specified, the 3D-DIC system with two cameras is used in this work.

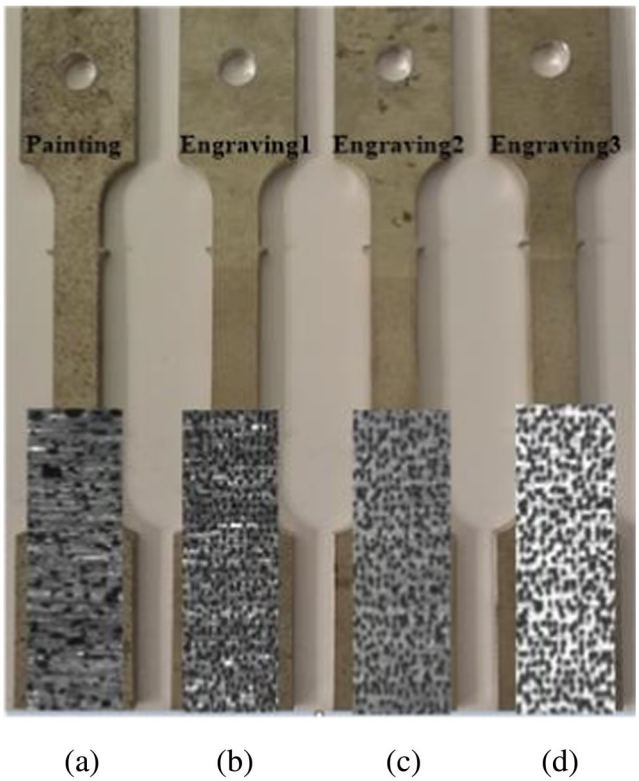

Fig. 6 Speckles created by different methods: (**a**) spray-painted speckles; (**b**) laser-engraved speckles with a depth of 59 μm; (**c**) laser-engraved speckles with a depth of 68 μm; (**d**) laser-engraved speckles with a depth of 75 μm

The shape of the specimen and the fixture are two important parts of a high-temperature mechanical experiment. Considering the convenience of clamping at high temperature, a dumbbell-type specimen and bolt-type fixtures are used in this work, as shown in Fig. 5(c).

Mechanical Properties of Titanium Alloy and Tungsten at High Temperatures

Verification of the Efficacy of the Laser Engraving Technique

Before we used the new technique to investigate the mechanical properties of various materials at different temperatures, we performed an experiment to ensure that the speckle pattern depth was quantitatively related to the error of the deformation measurement. The speckle depth on the surface of a specimen is related to the output power and exposure time of the laser engraving system. In this work, the exposure time is 0.1 ms. Four identical magnesium alloy specimens with dimensions of 190 mm×12.5 mm×4 mm, which were loaded in tension in an identical fashion, were used to study the effect of the speckle pattern depth related to the error of deformation measurement. One specimen had spray-painted speckles, whereas the others had laser-engraved speckles, as shown in Fig. 6. The localized

Table 2 Strain of the magnesium alloy specimens and relative errors

Speckle creating method	Depth /μm	Strain	Relative error
Painting	/	0.000551	7.4%
Engraving	59	0.000541	5.5%
	68	0.000524	2.1%
	75	0.000523	1.9%

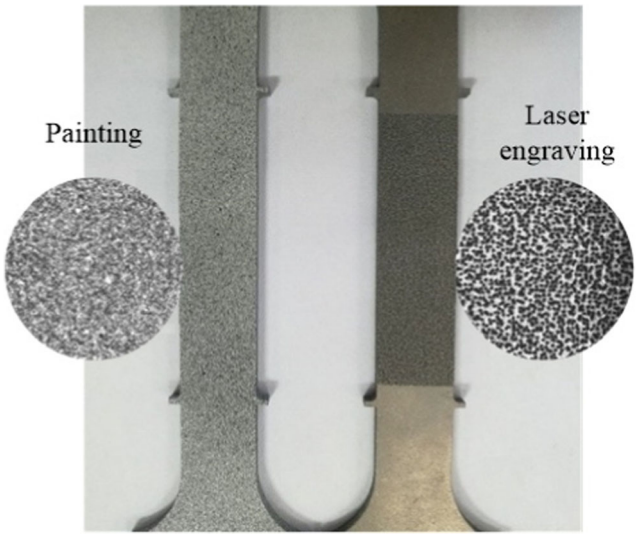

Fig. 7 Speckles created by painting and laser engraving

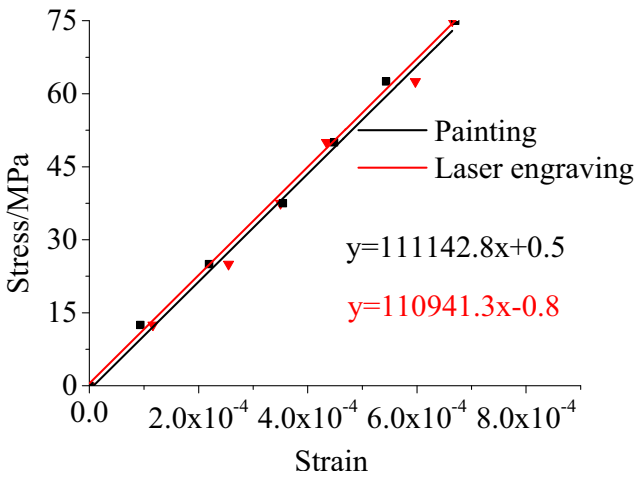

Fig. 9 Stress-strain relations of two Ti specimens: one with laser-engraved speckles and one with spray-painted speckles

and enlarged speckles in the figure show that the speckles created by the laser engraving system have high contrast and good uniformity. The depths of the three laser-engraved speckle patterns in this work are 59 μm, 68 μm, and 75 μm when the output powers of the laser engraving system are 5.91 W, 7.88 W, and 9.85 W, respectively. The dimensions of 100 randomly selected pits were measured on the surface of the laser-engraved speckles by using a metallurgical microscope with a fine focus knob, which was calibrated to 1 μm. The depths of the pits were measured by focusing on the specimen surface first at the lip of the pit and subsequently at the bottom of the pit, where the difference in fine focus knob reading is the pit depth.

The magnesium alloy specimens were preloaded at 500 N, and the load was 1000 N. During the experiment, the sample surface was illuminated by a high-power LED light through a quartz glass. Two CCD cameras of 2448×2048 pixel resolution and two Schneider Xenoplan lens of 1.9 / 35 mm were used to record the speckle pattern. The same lighting system and 3D digital image acquisition system were used in all the experiments, unless otherwise specified. According to an extensometer, the strain of the magnesium alloy specimen is 5.13×10^{-4} when the load is 1000 N. Table 2 lists the strain values of the magnesium alloy specimens obtained by 3D-DIC with different speckle patterns and the relative errors in comparison with the extensometer results. Table 2 shows that the results obtained by the speckles created by the laser engraving system have higher accuracy than the results from the speckles created by painting. Moreover, the testing results are more accurate with the increase in speckle depth, which can increase the contrast of the speckle pattern for light reflection in the pit of the speckle.

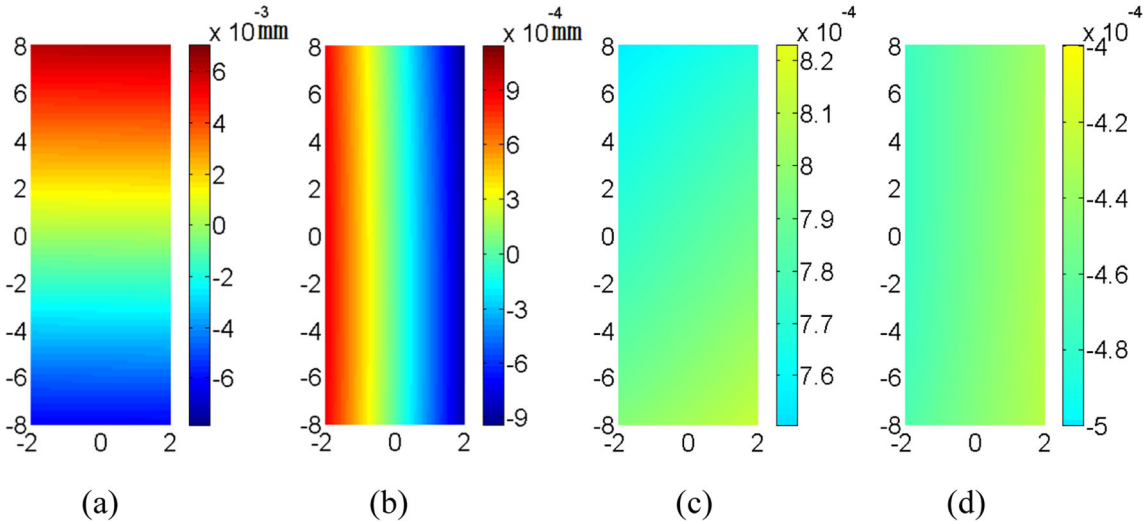

Fig. 8 Displacements and strains of the Ti alloy specimen with laser-engraved speckles obtained by DIC: (**a**) displacement along the *y* direction; (**b**) displacement along the *x* direction; (**c**) strain along the *y* direction; (**d**) strain along the *x* direction

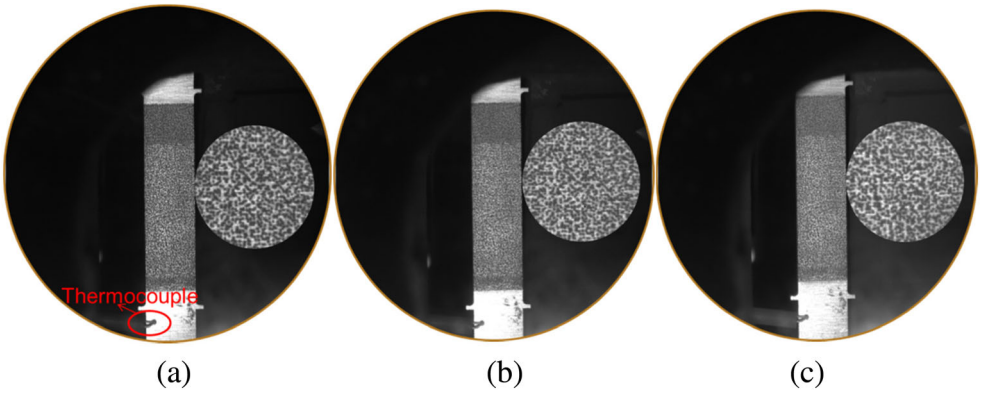

Fig. 10 Localized and enlarged speckles of the Ti alloy specimens at the following temperatures: (**a**) 600°C, (**b**) 650°C and (**c**) 700°C

Table 3 Measuring results obtained by 3D-DIC and the relative errors

Temperature	Sample	Displacement /mm	Relative error	Average relative error
600°C	1	0.0988	1.2%	1.37%
	2	0.0993	0.7%	
	3	0.1022	2.2%	
650°C	1	0.0959	4.1%	3.57%
	2	0.1040	4.0%	
	3	0.0974	2.6%	
700°C	1	0.1013	1.3%	2.50%
	2	0.1011	1.1%	
	3	0.0949	5.1%	

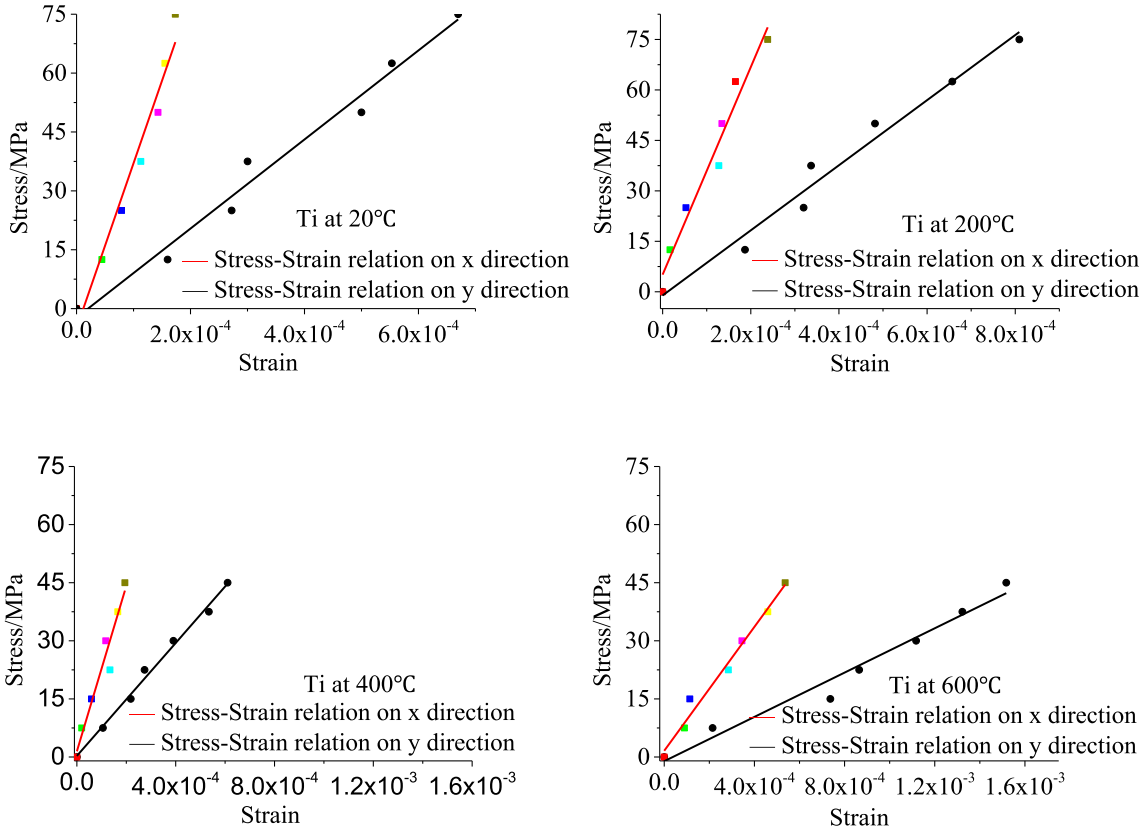

Fig. 11 Stress-strain relations of Ti specimens at different temperatures

Table 4 Elastic modulus and Poisson's ratio of Titanium alloy at different temperatures

Temperature	Sample	Elastic Modulus /GPa	Average Elastic Modulus /GPa	Poisson's Ratio	Average Poisson's Ratio
20°C	1	113.435	112.287	0.263	0.270
	2	111.139		0.277	
200°C	1	96.736	98.775	0.298	0.304
	2	100.813		0.310	
400°C	1	72.877	73.422	0.325	0.320
	2	73.966		0.315	
600°C	1	28.594	26.738	0.345	0.342
	2	24.881		0.338	

Another experiment was performed to ensure that the laser engraving process did not damage the specimen itself. We used two identical Ti alloy specimens with the dimensions of 190 mm×12.5 mm×3 mm and loaded them in tension in identical manners. One specimen had laser-engraved speckles, and the other had spray-painted speckles. The pictures of the two specimens are shown in Fig. 7. The gray values of the area with speckles are approximately 180~210, and the gray values of the area without speckles are approximately 48~50. The average engraving depth on the Ti alloy specimen is approx-

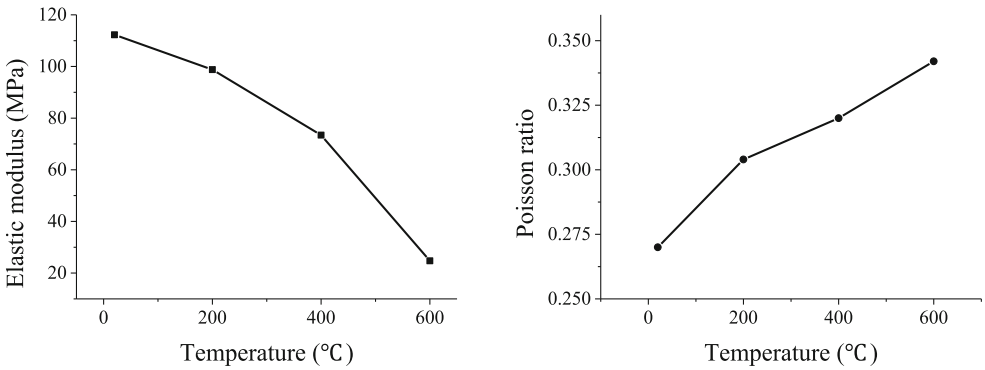

Fig. 12 Elastic modulus and Poisson's ratio vs temperature

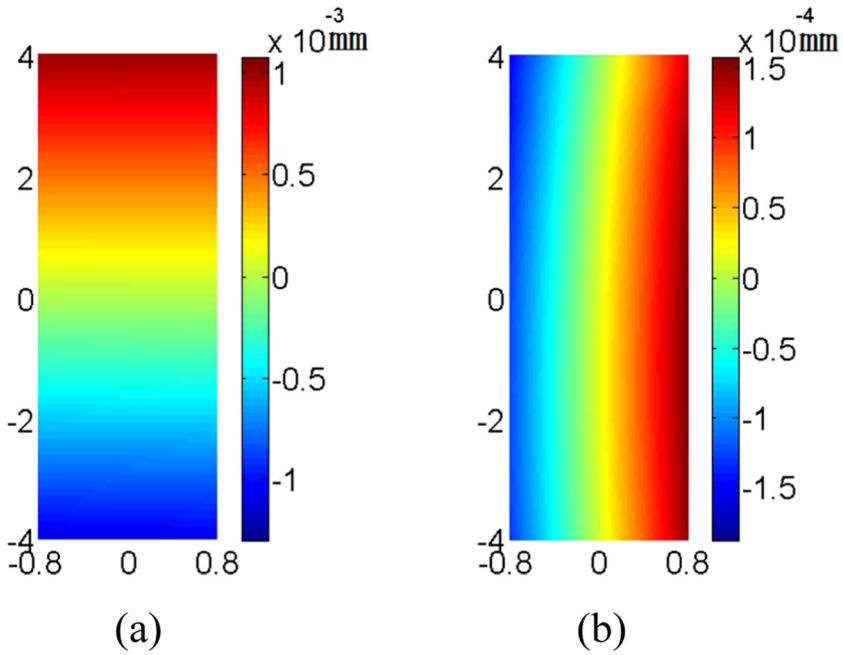

Fig. 13 Displacement field of the tungsten specimen with laser-engraved speckles at room temperature along the (**a**) *y* direction and (**b**) *x* direction

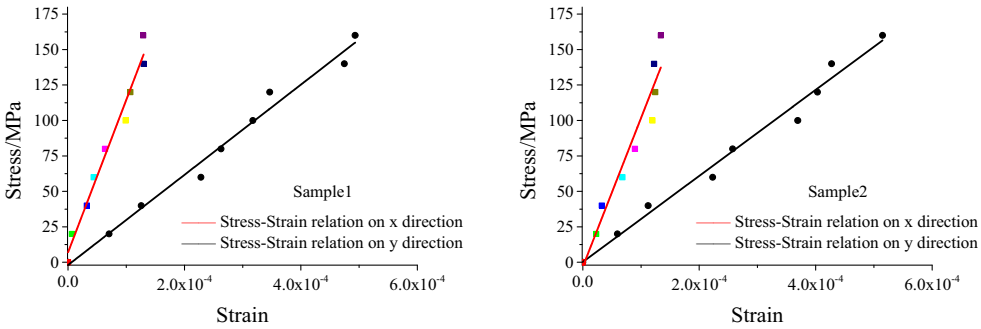

Fig. 14 Stress-strain relations of the tungsten samples at room temperature

imately 70 μm, and the standard deviation is 5.35 μm. Both specimens were loaded stepwise in uniaxial tension, and the experiments were repeated once at room temperature. The preload of the titanium alloy specimen was 500 N, and the maximum load was 3000 N. The loading rate was 0.1 mm/min. The displacement and strain contours of the Ti alloy specimen with laser-engraved speckles obtained by 3D-DIC are shown in Fig. 8, where the load was 3000 N. The y-axis is the direction of stretching, and the x-axis is perpendicular to the direction of stretching in all the experiments, unless otherwise specified. The stress-strain relations of the two Ti specimens, which are plotted in Fig. 9, are essentially identical: the Young's moduli of the Ti alloy specimens obtained by different speckles are 111.14 GPa and 110.94 GPa (the relative error is 0.18%). Encouraged by this result, we proceeded to perform high-temperature tests with the titanium alloy and tungsten specimens.

Determination of the Elastic Moduli and Poisson's Ratios of Titanium Alloy at Different Temperatures

The Ti alloy specimens with laser-engraved speckles were selected to demonstrate our system operation at high temperature. Before we proceeded to use 3D-DIC to investigate the mechanical properties at high temperature, the effects of air refraction and the glass window in the optical path of the cameras were studied by a rigid motion displacement of a Ti alloy specimen at the following temperatures: 600°C, 650°C and 700°C. The Ti alloy specimen was hung on the upper end of the fixture, and one could move the specimen by 0.1 mm (the indication error of the measurement system is 0.5%). The speckle patterns of the Ti alloy specimens taken by the cameras at high temperature are shown in Fig. 10. The localized and enlarged speckles in the figures show that the speckles created by the laser engraving system have high contrast and good uniformity at high temperature. The measuring results obtained by 3D-DIC and the relative errors compared with the rigid body displacement of 0.1 mm are listed in Table 3. Table 3 provides evidence that the high-temperature-induced air refraction and the glass window in the optical path of the cameras have negligible effects on the 3D-DIC high- temperature measurement.

Next, the high-temperature mechanical properties of the Ti alloy specimen were studied using the high-temperature deformation measurement system and 3D-DIC with the laser-engraved speckles. The preload of the titanium alloy specimen was 500 N, and the maximum load was 3000 N, with a loading rate of 0.1 mm/min. We tested the specimens at the following temperatures: 20°C, 200°C, 400°C and 600°C. Each experiment was repeated once, and the stress-strain relations of the first Ti alloy specimen are shown in Fig. 11, where the stress is defined as the tensile load divided by the original cross-sectional area of the specimen. The average result of Young's moduli and Poisson's ratios are listed in Table 4.

The results show that when the temperature increases, the elastic modulus decreases. The rate of the decrease appears to be enhanced by the increasing temperature.

Table 5 Elastic moduli of tungsten at room temperature

Measurement sample	Elastic modulus /GPa	Poisson's ratio
Sample 1	318.008	0.289
Sample 2	303.604	0.278
Standard value	313±20	/

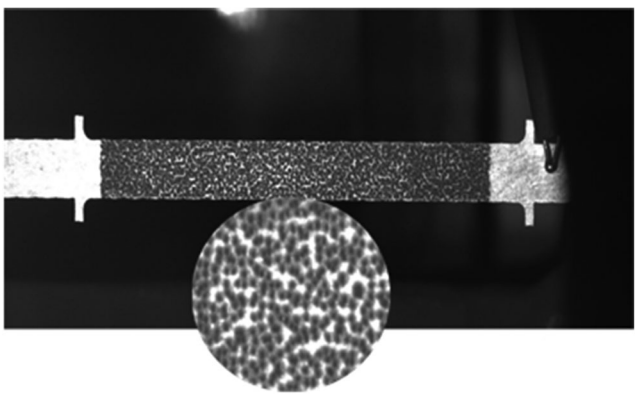

Fig. 15 Laser-engraved speckle pattern of tungsten at 1000°C

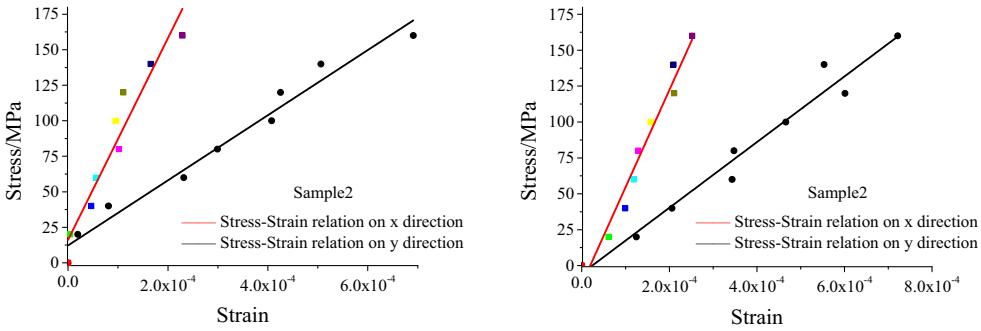

Fig. 16 Stress-strain relation of tungsten at 1000°C, as obtained from the laser-engraved speckle pattern

The relationship between the temperature and the elastic modulus is plotted in Fig. 12.

Measurement of the Elastic Moduli of Tungsten Samples at 1000°C

First, we tested the tungsten specimens at room temperature. Two standard tungsten tension specimens with dimensions of 190 mm×5 mm×0.5 mm were manufactured. The average engraving depth of the tungsten specimen is approximately 25 μm, and the standard deviation is 4.58 μm. A preload of 50 N was applied to secure the specimen. Then, a stepwise 50 N load was added until a maximum load of 400 N was attained. The rate of loading was 0.06 mm/min. The corresponding displacement contour of each speckle pattern was calculated using the 3D-DIC software, as shown in Fig. 13 at 100 N. The stress-strain relations along the x and y directions of the tungsten specimens are shown in Fig. 14. The corresponding results are listed in Table 5. Thus, the obtained Young's moduli of the tungsten samples are 318 GPa and 304 GPa, which are notably close to the published value of 313±20 GPa [23].

Next, we determined the mechanical properties of tungsten at 1000°C. The experiments were performed with identical steps to the aforementioned processes, and two standard tension specimens were used. The laser-engraved speckle pattern of tungsten at 1000°C is shown in Fig. 15. The stress-strain relations along the x and y directions at 1000°C on the tungsten specimens are shown in Fig. 16. The elastic moduli and Poisson's ratios of the tungsten samples at 1000°C are listed in Table 6. The average elastic modulus of the tungsten samples at 1000°C is 229 GPa, which is notably smaller than that at room temperature.

Table 6 Elastic moduli of tungsten at 1000°C

Measurement sample	Elastic modulus /GPa	Poisson's ratio
Sample 1	229.266	0.306
Sample 2	228.650	0.335

Conclusion

In this paper, we have presented a new technique to produce high-temperature speckle patterns on metals. The advantage of this technique is that the size and distribution of the speckles can be varied at will. We have applied this technique to determine the high-temperature Young's modulus of titanium at 1000°C and the Young's modulus of a titanium alloy at 20°C, 200°C, 400°C and 600°C. The results show that the Young's modulus of the titanium alloy decreases when the environmental temperature increases. We believe that this technique can be applied to nonmetal materials, such as FRP and indium oxide, and to the curved surfaces of materials. However, special care should be exercised when the technique is applied to notably thin materials to avoid changing their intrinsic properties.

References

1. Peters WH, Ranson WFJ (1982) Digital image techniques in experimental stress analysis. Opt Eng 21(3):427–431
2. Yamaguchi IJ (2000) A Laser Speckle Strain gage. J Phys E Sci Instrum 14(11):1270. https://doi.org/10.1088/0022-3735/14/11/012
3. Chiang FP, Kin CCJ (1983) Some optical techniques of displacement and strain measurements on metal surfaces. Jom-J Min Met Mat S 35(5):49–54. https://doi.org/10.1007/BF03338279
4. Cheng JB, Chiang FPJ (1984) Statistical analysis of whole field filtering of specklegram and its upper limit of measurement. J Opt Soc Am A 1(8):845–849. https://doi.org/10.1364/JOSAA.1.000845
5. Jiang C, Wu YF, Jiang JF (2017) Effect of aggregate size on stress-strain behavior of concrete confined by fiber composites. Compos Struct 168:851–862
6. Jiang C, Wu YF, Wu G (2014) Plastic hinge length of FRP-confined square RC columns. J Compos Constr 18(4):04014003
7. Cheng JB, Chiang FPJ (1987) Fringe formation of shearing speckle interferometry. Proc SPIE 0814:124–128. https://doi.org/10.1117/12.941684
8. Creath K, Slettemoen GAJ (1985) A vibration-observation techniques for digital speckle-pattern interferometry. Opt Sot Am A 2(10):1629–1636
9. Baik S-H, Park S-K, Kim C-J, Kim JS-Y (2001) Two-channel spatial phase shifting electronic speckle pattern interferometer.

Opt Commun 192(3–6):205–211. https://doi.org/10.1016/S0030-4018(01)01223-8
10. Slangen P, Berwart L, Veuster CD, Golinval J-C, Lion YJ (1996) Digital speckle pattern interferometry (DSPI): a fast procedure to detect and measure vibration mode shapes. Opt Lasers Eng 25(4–5):311–321. https://doi.org/10.1016/0143-8166(95)00078-X
11. Pan B, Xie HM, Hua TJ (2009) Measurement of coefficient of thermal expansion of films using digital image correlation method. Polym Test 28(1):75–83. https://doi.org/10.1016/j.polymertesting.2008.11.004
12. Wang YG, Tong WJ (2013) A high resolution DIC technique for measuring small thermal expansion of film specimens. Opt Lasers Eng 51(1):30–33. https://doi.org/10.1016/j.optlaseng.2012.08.001
13. Cheng JB, Yu X, Miller RG, Feng ZJ (2014) In situ strain and temperature measurement and modelling during arc welding. Sci Technol Weld Join 20(3):181–188. https://doi.org/10.1179/1362171814Y.0000000270
14. Volkl R, Fischer BJ (2004) Mechanical testing of ultra-high temperature alloys. Exp Mech 44(2):121–127. https://doi.org/10.1007/BF02428171
15. Meyer P, Waas AMJ (2015) Measurement of In Situ-Full-Field Strain Maps on Ceramic Matrix Composites at Elevated Temperature Using Digital Image Correlation. Exp Mech 55:795–802. https://doi.org/10.1007/s11340-014-9979-7
16. Lyons JS, Liu J, Sutton MAJ (1996) High-temperature deformation measurement using digital image correlation. Exp Mech 36(1):64–70. https://doi.org/10.1007/BF02328699
17. Ma S, Pang J, Ma Q (2012) The systematic error in digital image correlation induced by self-heating of a digital camera. Meas Sci Technol 23(2):025403. https://doi.org/10.1088/0957-0233/23/2/025403
18. Pan B, Wu DF, Gao JXJ (2014) High-temperature strain measurement using active imaging digital image correlation and infrared radiation heating. J Strain Anal Eng 49(4):224–232. https://doi.org/10.1177/0309324713502201
19. Seldes AM, Arabehety CGJ (1998) Experimental Characterization of Crack Tip Deformation Fields In Alloy 718 At High Temperatures. J Eng Mater Technol 120(1):71–78. https://doi.org/10.1115/1.2806840
20. Su YQ, Yao XF, Wang S, Ma YJJ (2015) Improvement on measurement accuracy of high-temperature DIC by grayscale-average technique. Opt Lasers Eng 75:10–16. https://doi.org/10.1016/j.optlaseng.2015.06.003
21. Grant BMB, Stone HJ, Withers PJ, Preuss MJ (2009) High-temperature strain field measurement using digital image correlation. J Strain Anal Eng Des 44(4):263–271. https://doi.org/10.1088/1361-6501/aa56d1
22. Xu C, Xu N, Yang L, Xiang D (2012) High temperature displacement and strain measurement using a monochromatic light illuminated stereo digital image correlation system. Meas Sci Technol 23(2012):125603
23. Song GM, Wang YJJ (2001) Microstructures and Mechanical Properties of ZrCp/W Composites at Room Temperature. Rare Metal Mater Eng 30(6):448–452 https://www.researchgate.net/publication/290581195